Soret effect of *n*–Octyl β–D–glucopyranoside (C_8G_1) in water around the critical micelle concentration

Bastian Arlt,[†] Sascha Datta,[‡] Thomas Sottmann,[*,‡] and Simone Wiegand[*,†]

Institute of Solid State Research - Soft Matter, Forschungszentrum Jülich, Jülich, Germany, and Department of Chemistry, University of Cologne, Cologne

E-mail: thomas.sottmann@uni-koeln.de; s.wiegand@fz-juelich.de

Abstract

We studied the thermal diffusion behavior of the nonionic surfactant C_8G_1 (*n*–Octyl β–D–glucopyranoside) in water for different concentrations between w=0.25 wt% and w=2.0 wt% in a temperature range from T=15 °C to 60 °C using the classical and infrared thermal diffusion forced Rayleigh scattering (TDFRS) setup.

The purpose of the present paper is the investigation of the thermal diffusion behavior of surfactant systems around the critical micelle concentration (*cmc*), which is independently determined by surface tension measurements. In the classical TDFRS the surfactant solutions show in the presence of a light absorbing dye a pronounced change of the thermal diffusion coefficient (D_T) and the Soret coefficient (S_T) at the *cmc*. This result agrees with a recent thermal lens study [Santos *et al.*, *Phys. Rev. E* **2008**, 77, 011403], which also showed in the presence of dye a pronounced change of the thermal lens matter signal around the *cmc*. We found that this change becomes less pronounced, if the dye is absent or a light source is used, which is not absorbed by the dye. At higher concentrations we observed a temperature dependent sign change of S_T as it has also been found for solutions of hard spheres at higher concentrations.

[*]To whom correspondence should be addressed
[†]Institute of Solid State Research - Soft Matter, Forschungszentrum Jülich, Jülich, Germany
[‡]Department of Chemistry, University of Cologne, Cologne

Introduction

Surfactant molecules, which show amphiphilic properties due to their hydrophilic head and hydrophobic tail, form micelles in water, when the concentration of the monomer is above a critical micelle concentration (*cmc*). The size, shape and structure of the micelles depend on concentration, temperature and the molecular structure of the surfactant.[1,2] Surfactant solutions are of great interest due to their often complex phase behavior and their extensive applications.[3–7] Over the last years sugar surfactant systems have been investigated experimentally and theoretically.[8–11] These biocompatible surfactants have frequently been used to study the dissolution and formation of biological membranes and the stabilization of proteins.[12–16]

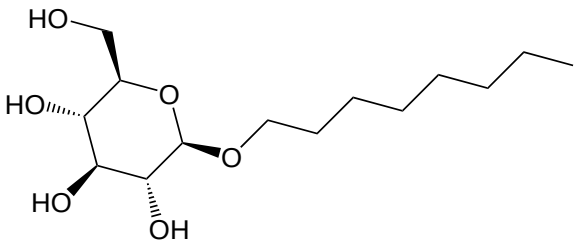

Figure 1: Molecular structure of β–C_8G_1.

Thermal diffusion describes the mass transport of components due to a temperature gradient. As a result of this process a formation of a concentration gradient can be observed. In the steady state when the mass flux vanishes, the concentration gradient is given by

$$\nabla w = -S_T w(1-w)\nabla T. \tag{1}$$

The Soret coefficient $S_T = D_T/D$ is defined as the ratio of the thermal diffusion coefficient D_T and the translational diffusion coefficient D. w is the weight fraction of the component with higher molar mass. Due to the fact that the Soret coefficient is inversely proportional to the translational diffusion coefficient, S_T is larger for slow diffusing systems like heavy and large polymers and colloids compared to low molecular weight mixtures.[17–21] In contrast, the size and shape dependence of D_T is not so pronounced: for instance, it is well known that D_T is independent of the molecular

mass and shape for diluted solutions of polymers.[22] A similar tendency has recently been observed for higher alkanes.[23]

Several experimental techniques have been used to study the thermal diffusion behavior of surfactant systems. Piazza *et al.* investigated an ionic surfactant, sodium dodecyl sulphate (SDS), in water using a beam deflection and thermal lens setup.[24,25] They found that S_T increases with increasing salt concentration due to the strong influence of intermicellar interactions. They investigated also the nonionic surfactant β-dodecyl maltoside ($C_{12}G_2$), which has the same hydrophobic tail as SDS and two glucose rings as head group. $C_{12}G_2$-micelles showed a strong tendency to move to the cold region, which might be caused by the interaction of the surface of micelles with the solvent via hydrogen bonds. Ning *et al.* studied a series of nonionic surfactants in water in a wide temperature and concentration range using the thermal diffusion forced Rayleigh scattering (*TDFRS*) technique.[26,27] For their measurements a small amount of an ionic dye (Basantol® Yellow) is added in order to create a sufficient temperature gradient. The measurements show that the addition of the dye influences the thermal diffusive behavior considerably, therefore the infrared–TDFRS (*IR–TDFRS*) setup has been developed to avoid the addition of dye for aqueous systems.[28]

Santos *et al.* investigated the Soret coefficient of potassium laurate in water and found an abrupt change of the matter lens signal at the *cmc*.[29] Unfortunately, an evaluation of S_T was not possible due to the presence of the dye which complicated the analysis. Therefore, it remained unclear to which extend the *cmc* is also visible in the thermal diffusion, diffusion and Soret coefficient. To clarify these observations the thermal diffusion behavior of micellar systems with a high *cmc* needs to be investigated without the addition of dye.

Among the wide range of surfactants we found nonionic sugar surfactants with a fairly high *cmc*, such as *n*–Octyl β–D–glucopyranoside, in the following referred to as C_8G_1.[30] The β–form has a linear molecular structure which is shown in Figure 1. Additionally, an α–*L*–form exists, which differs in the linkage between the hydrophilic head and the hydrophobic chain of the alkyl glucoside,[31,32] but this less common α-form will not be considered in the present work.

Many properties such as the phase and structural behavior, the influence of salt, but also the so-

lute/solvent interactions have been studied for aqueous solutions of C_8G_1.[31,33,34] From previous studies on aqueous systems[21,35] we know that the solute/solvent interaction and the capability to form hydrogen bonds often influences the thermal diffusion behavior. Pastor *et al.*[33] determined the number of water molecules (*hydration number*), surrounding the C_8G_1 molecules. They found a hydration number of 16 for monomers below the *cmc*, which is decaying exponentially above the *cmc* to 8 for concentrations around 1.5 wt%, while at the same time the aggregation number increases from 54±5 to 104±5 when increasing the concentration from 0.85 to 1.5 wt%. They also observed a slight shift of the *cmc* to lower concentrations when adding salt. Based on their results they assumed spherical micelles at low micellar concentrations which turn to more asymmetric forms (i.e., elliptical forms) at higher concentrations.

In this work, we determine the *cmc* of C_8G_1 in water in a temperature range between T=15 °C and 40 °C by surface tension measurements and study the thermal diffusion of the system using both, the classical TDFRS as well as the IR–TDFRS. The classical TDFRS has been used to study the system in the presence of dye as it was also done in the work by Santos *et al.*.[29] Therefore, we had also to investigate to which extent the *cmc* is shifted in the presence of the trivalent dye Basantol®Yellow. In order to gain a better understanding of the influence of the dye on the transport properties we performed experiments with the IR–TDFRS without and also in the presence of dye.

Experiment and data analysis

Sample preparation and characterization

n–Octyl β–D–glucopyranoside (abbreviated as C_8G_1, $C_{14}H_{28}O_6$, M = 292.38 g mol^{-1}) was purchased from Glycon Biochemicals (Germany) with a purity of 99.5%. A phase diagram of the aqueous surfactant system H_2O – C_8G_1 (without dye) was recorded by Nilsson *et al.*[31] and is shown in Figure 2.

All samples are prepared by weighting with the accuracy of the balance (±0.0001 g) using

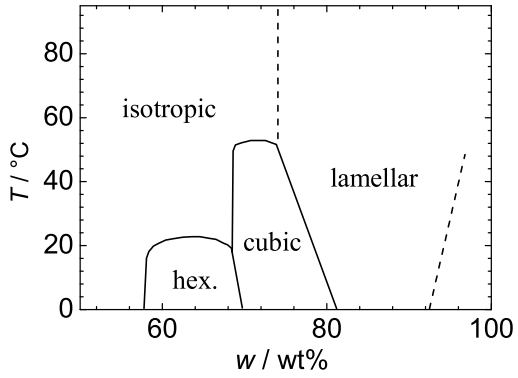

Figure 2: Phase diagram of C_8G_1, redrawn from Nilsson *et al.*[31]

deionized Milli-Q water. In the classical TDFRS setup we used a tiny amount of the ionic dye Basantol®Yellow (BASF).[36] The optical density was adjusted to 2 cm^{-1} at a wavelength of λ = 488 nm using a Carry 50 spectrometer. For the absorption measurements we use cells with a thickness of 1 mm. For the IR–TDFRS and classical TDFRS measurements, the surfactant solutions are directly filtered into the sample cell by a PTFE (Roth) filter with a mesh size of 5μm. The Hellma sample cells used for both TDFRS experiments have a thickness of 0.2 mm.

For conversion of the molar fractions into weight fractions we used a density of C_8G_1 of 1.13 g/cm^3, which is an approximation by Stubenrauch *et al.*,[37] based on data by Nilsson *et al.*[31] at T = 25 °C.

Determination of the critical micelle concentration

The critical micelle concentration has been determined by surface tension measurements, which were performed with a Krüss digital tensiometer K10T. Concentration series of the C_8G_1/water mixture at *T*=15 °C, 20 °C, 30 °C and 40 °C have been measured. The dye-containing mixtures have been studied at *T*=23 °C and 30 °C, respectively. The temperature was controlled with an accuracy of ±0.1 K.

The trend of the surface tension versus the logarithm of the concentration can be described by the Langmuir–Szyszkowski–equation[38] below the *cmc* (Figure 3). Above the *cmc*, the surface tension

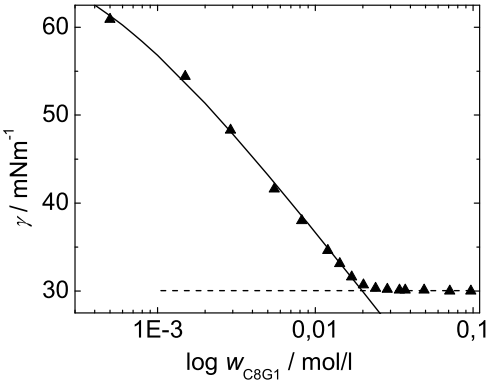

Figure 3: Surface tension (γ) of the binary system H_2O / C_8G_1 as function of the concentration at T=30 °C. The continuous line marks the fit with the Langmuir–Szyszkowski equation at low concentrations, the linear fit (dashed line) was drawn for the seven highest concentrations. The intersection point marks the *cmc*.

is almost constant, thus this range can be fitted linearly. The intersection of both curves marks the *cmc*.

Classical TDFRS and IR–TDFRS measurement

The IR–TDFRS[28] and the classical TDFRS[27] setup have been described elsewhere in detail. In both setups an optical grating is written into the sample by intersecting two laser beams with a wavelength of 980 nm or 488 nm, respectively. Due to a weak absorption band of water at 980 nm no dye is required for aqueous systems in the IR–TDFRS setup. Contrarily we need to add a small amount of dye in the classical TDFRS to achieve a sufficient absorption at 488 nm. In both setups the optical grating is converted into a temperature grating, which results in a refractive index grating. This grating diffracts a He–Ne laser beam at λ=633 nm.

Especially for aqueous mixtures, it has turned out that it is difficult to find an inert dye, which does not influence the experiment. Water soluble dyes often change their absorption behavior with *pH* or temperature.[39,40] In complex systems the addition of dye can also influence the phase behavior and microstructure of the micellar system and also their thermal diffusion behavior.[41]

For all experiments, the sample cell is thermostated in a brass or copper holder for at least

half an hour. The temperature of the holder is controlled by a circulating water bath (Lauda E300 thermostat) with an accuracy of ± 0.02 K. The classical TDFRS and IR–TDFRS measurements are performed in a concentration range between w_{C8G1}=0.25–2.0 wt% and T=15 °C to 40 °C, and for chosen samples in a temperature range up to 60 °C.

Data analysis

The normalized diffraction signal ζ_{het} is described by

$$\zeta_{het}(t) = 1 + \left(\frac{\partial n}{\partial T}\right)_{w,p}^{-1} \left(\frac{\partial n}{\partial w}\right)_{T,p} \cdot S_T w(1-w)\left(1 - e^{-q^2 D t}\right), \tag{2}$$

where q is the scattering vector. The refractive index increment $(\partial n/\partial w)_{p,T}$ at constant pressure and temperature has been measured with a refractometer (Anton Paar). Five measurements are done for each concentration to reduce the error bars.

For the determination of $(\partial n/\partial T)_{p,w}$ at constant pressure and surfactant weight fraction an interferometer has been used. In general, the $(\partial n/\partial T)_{p,w}$ measurements of C_8G_1 solutions as function of surfactant weight fraction were done between T=15 °C and 40 °C. For a few weight fractions we performed measurements up to T=60 °C. $(\partial n/\partial T)_{p,w}$ decreases reciprocally proportional with increasing temperature.

According to Rosen[42] and Preston[43] it should also be possible to determine the critical micelle concentration from the variation of the refractive index with concentration. However, measuring the refractive index as function of concentration we found an almost perfect linear concentration dependence, which makes it impossible to determine the *cmc*. To our knowledge, the refractive index measurements are not favored for the *cmc* determination of C_8G_1 in H_2O which shows a fairly high *cmc*. Instead, Strop and Brunger[44] used refractive index measurements for the determination of the surfactant concentration in solution for aqueous systems with low *cmc* values, namely polyoxyethylene(8)dodecyl ether ($C_{12}E_9$, $c_{cmc} = 100\mu M$[45]) and *n*–dodecyl–β–D–maltopyranoside

($C_{12}G_2$, c_{cmc} = 230μM[46]). They found a linear relationship between the change of the refractive index with surfactant concentration in the measured concentration range. But they expect, that this method can also be applied for high *cmc* systems using lower-sensitivity detectors.

Results and discussion

Surface tension measurements

As already described we determined the critical micelle concentration by surface tension measurements. The temperature dependence of the *cmc* is shown in Figure 4. We studied two different batches of C_8G_1: an old batch (rectangles) (Glycon, 2005) and a new one (circles) (Glycon, 2008). We found systematically larger *cmc* values for the new batch, however this difference could be explained with a changed workup method in the production process (notice by manufacturer). Anyway, the temperature-dependence of the *cmc* is qualitatively the same for both batches. To avoid misunderstanding, we performed all TDFRS measurements with the new C_8G_1 batch.

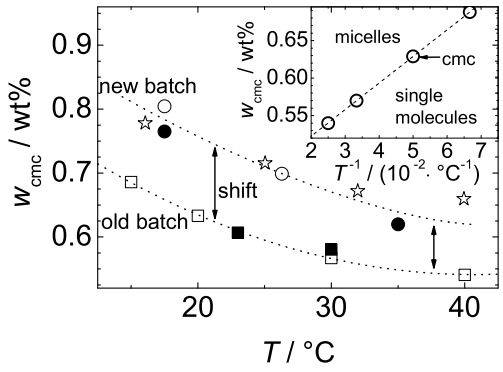

Figure 4: The *cmc* for C_8G_1/water was determined by surface tension measurements without (○, □) and with dye (●, ■) for the old (□, ■) and the new surfactant batch (○, ●), and compared with literature values by Aoudia and Zana[47] (☆). The error bars are in the order of the symbol size. Inset: *cmc* as function of the inverse temperature in Celsius. The dashed line is a linear fit to the data points.

For both batches we observe a decay of the *cmc* with increasing temperature. This can be explained with a decreasing hydrophilicity of the surfactant molecules with increasing temperature

due to the decreasing ability to form hydrogen bonds. Typically the *cmc* of nonionic surfactants passes through a minimum and increases at higher temperatures again.[47,48] In the investigated temperature range up to T=40 °C we did not observe the minimum and the final increase, but Aoudia and Zana[47] observed a shallow minimum around T=42 °C for the same surfactant system. A fit of our data (dashed line in Figure 4) shows, that we can expect a similar temperature for the minimum *cmc*. The position of the minimum is determined by the size of the head group, which is fairly large in the case of the sugar surfactant. Also for different polyoxyethylene glycol mono–dodecylethers $C_{12}E_j$ with oxyethlyene chain lengths of $j = 4,\ 6$ and 8 a shift of the minimum from T=40 °C to T=50 °C has been observed.[48]

To investigate the influence of the ionic dye Basantol®Yellow on the *cmc* we performed measurements with a concentration of Basantol®Yellow of $c = 1.5 \times 10^{-4}$ M (full circles and full rectangles in Figure 4), corresponding to the dye-concentration in the TDFRS experiments. At this rather low concentration we do not see a significant influence of Basantol®Yellow. Pastor *et al.* found a change of the *cmc* of C_8G_1 in water of 10-15% adding 0.05 M $CaCl_2$ or $ZnCl_2$.[33] Since the dye concentration in our experiments is about two orders of magnitude smaller we would expect only a change of the *cmc* in the sub-percent range, which is in agreement with our results.

Thermal diffusive behavior around the *cmc*

Below the *cmc*, the surfactant molecules in solution are in equilibrium with those adsorbed at the water/air interface. Above the *cmc* also micelles are formed in the solution. Therefore, we will observe the thermal diffusion behavior of the individual surfactant molecules below the *cmc*, while above the *cmc* we have additionally a thermophoretic motion of the micelles. This might also lead to a pronounced change of the thermal diffusion or Soret coefficient.

For the surfactant system under study the determined Soret coefficients correspond to an averaged value. We can not differentiate between the contribution stemming from the C_8G_1 molecules and micelles, as it can be done for a polymer in a solvent mixture.[35] In the latter case the diffusion process of the solvent mixture and the polymer can be differentiated, because the time constants of

the two processes differ by more than one order of magnitude. For the micellar solution the time constants of the single molecules and the micelles are so close that we can not separate the two processes in the experimental signal. Therefore, we observe only an averaged value, which describes the thermal diffusion motion of C_8G_1 in water and depending on the location in the phase diagram the signal can be a superposition of different contributions. A detailed analysis of the different contributions in a phenomenological approach suggested by Santos *et al.* is not possible.[29]

In the following we compare the results of both TDFRS setups in order to determine the influence of the dye. In Figure 5 we show the temperature dependence of the Soret coefficient, the thermal diffusion coefficient and diffusion coefficient for a sample with a surfactant concentration of w=0.6 wt% where we found the *cmc* at T=23 °C. In the plot we display data obtained with the IR–TDFRS and the classical TDFRS. In the latter case the samples contain Basantol®Yellow as dye. Additionally, we performed measurements with the IR–TDFRS in the presence of dye.

The diffusion coefficient D and the thermal diffusion coefficient D_T increase continuously with temperature. None of the diffusion coefficients shows a noticeable change at the *cmc*. The difference of D obtained with the different setups is almost negligible although D obtained with the classical setup is systematically larger, which might indicate smaller micelles or attractive interactions. In our case the addition of the dye leads to charged micelles, which repel each other and which should lead to slower dynamics.[49,50] Surprisingly, in our case the diffusion becomes faster, when the micelles are charged (middle chart in Figure 5). This might be explained by an inhomogeneous heating of the dye-containing micelles, which leads to a faster movement.

The temperature dependent slope of D_T measured with the classical TDFRS is larger than the one measured without dye in the IR–TDFRS. We assume that the dye is incorporated into the micelles and the interfacial energy of the micelles changes. This assumption is supported by the fact that the molar fraction of the dye molecules and micelles is in the same order of 1.5×10^{-4} mol/L, if we take into account the aggregation numbers determined by Pastor *et al.*[33] The incorporation of the dye into the micelles influences also the diffusion coefficient. The reason could be either that the interaction energy changes due to a modified interfacial energy or that the shape is modified. The

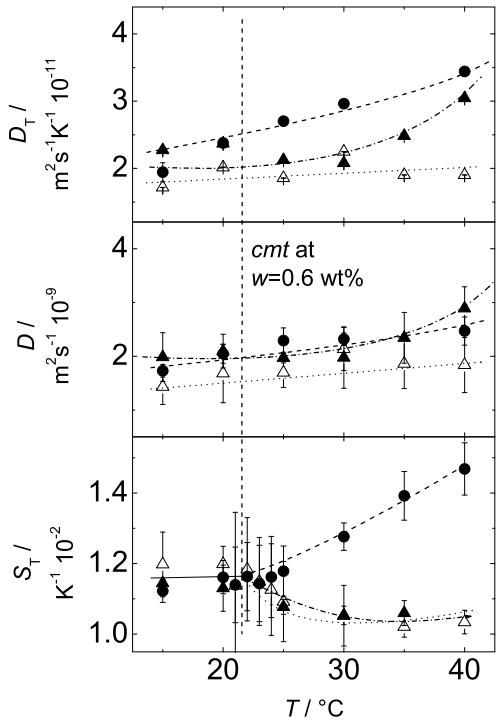

Figure 5: Comparison of S_T, D_T and D as function of the temperature for w=0.6 wt% in the IR (△ (without dye), ▲ (with dye)) and the classical TDFRS (●). Bottom: above the *cmt* we observe larger S_T–values in the classical TDFRS than in the IR–TDFRS. Independent of the method or the presence of the dye we find the same Soret coefficients below the *cmt* of T=23 °C within the error bars of approximately 10%.

latter we will have to confirm by neutron scattering experiments.

Below the *cmc* all Soret coefficients agree within their error bars and S_T is temperature independent (cf. Figure 5). For temperatures above the *cmc* we observed, that the Soret coefficient for the classical setup is larger compared to the IR setup.In the classical TDFRS the incorporation of the dye in the micelles probably induces a stronger local heating, which modifies the thermal diffusion behavior strongly. This was probably also the reason leading to the abrupt change of the thermal lens signal of the aqueous potassium laurate solution with Congo red.[29] We suspect that it is really necessary to create the thermal grating with the absorbing wavelength, because recent experiments on a nonionic surfactant with Basantol®Yellow as dye[41] showed that homogeneous illumination with a blue laser in the IR–TDFRS does not have the same effect.

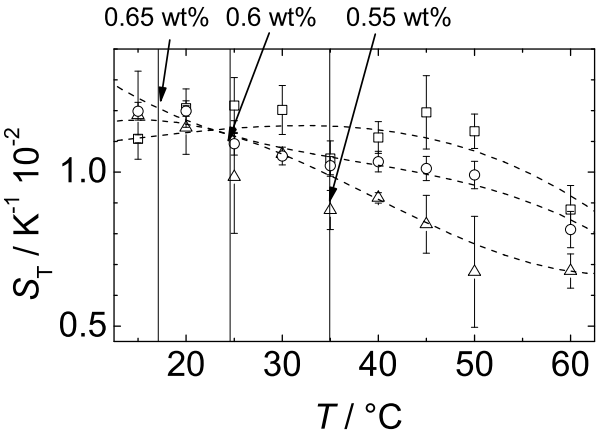

Figure 6: The Soret coefficient S_T as function of temperature determined with the IR–TDFRS without dye. For all concentrations (0.55 wt% (△), 0.6 wt% (○), 0.65 wt% (□)) the *cmt* lies between T=15 °C and 40 °C. The dashed lines are guides to the eyes and the arrows mark the *cmt* for the various concentrations.

In Figure 6 the temperature dependence of the Soret coefficient is plotted for three different concentrations, which have their *cmt*s in the investigated temperature range. For each concentration we marked the *cmt* by an arrow. For none of the concentrations it is possible to determine the *cmt* from the Soret measurements. In this plot we display also the IR–TDFRS measurement for a concentration of 0.6 wt%, which had already been displayed in Figure 5 (bottom chart), but without the measurement of the classical TDFRS, which gives a clear indication of the *cmt*. We conclude

that the temperature dependent measurement of S_T obtained by the IR–TDFRS does not show an unmistakable change in the shape of the curve in order to determine the *cmt*. In order to see a clear effect some dye needs to be added and a light source has to be used, which is absorbed by the dye.

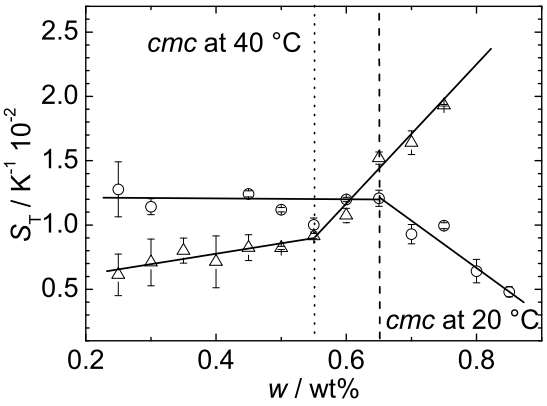

Figure 7: The Soret coefficient S_T at constant temperature versus concentration at 20 °C (○) and 40 °C (△). All measurements have been performed with the IR–TDFRS without dye. The vertical lines mark the *cmc* at 20 °C (dashed) and 40 °C (dotted). The solid lines are guides to the eye.

In contrast, we are able to determine the *cmc* by plotting the Soret coefficient over the sugar surfactant concentration as shown in Figure 7. For both temperatures the slope of the Soret coefficient changes clearly at the *cmc*. While the slope at 20 °C changes from zero to negative, the positive slope at 40 °C (dotted vertical line) becomes more pronounced above the *cmc*. For both temperatures below the *cmc* the concentration dependence of S_T is less pronounced. The measurements with the classical TDFRS setup do not give a better indication of the *cmc*. For clarity the data have not been displayed. The obtained *cmc* values are in good agreement with the results from the surface tension measurements.

Results for higher concentrated solutions

We also investigated the thermal diffusion behavior for higher surfactant concentrations. Figure 8 shows the thermal diffusion D_T, diffusion D and Soret coefficient S_T as function of concentration for different temperatures.

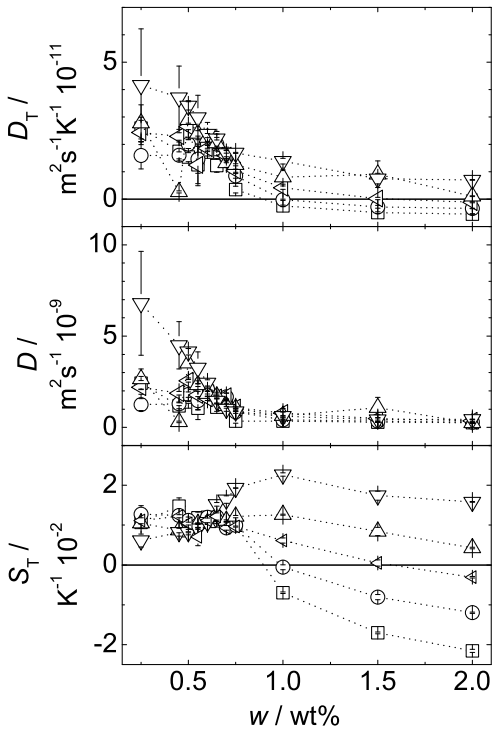

Figure 8: The thermal diffusion D_T, diffusion D and Soret coefficient S_T as function of concentration for different temperatures 15 °C (□), 20 °C (○), 25 °C (◁), 30 °C (△), 40 °C (▽).

For all temperatures the thermal diffusion coefficient D_T decreases with increasing surfactant concentration and with decreasing temperature (cf. top of Figure 8). For the three lower temperatures of T=15 °C, 20 °C and 25 °C a sign change occurs at a concentration of w=0.9 wt%, 1.0 wt% and 1.6 wt%, while D_T stays positive at higher temperatures. The decay of D_T becomes weaker for higher concentrations. As can be seen in the middle part of Figure 8 the diffusion coefficient D decreases for lower concentrations, while above the *cmc* the diffusion is almost independent of the concentration.

In the bottom part of Figure 8 the concentration dependence of the Soret coefficient is shown for different temperatures. S_T passes through a maximum for T=20 °C and T=40 °C before it is decaying almost linearly above a concentration of w =1.0 wt%. By decreasing the temperature this decay becomes steeper. For the two highest temperatures 30 °C and 40 °C we did not observe a sign change in the investigated concentration range, but it is expected that it will occur at higher concentrations.

The decay of the Soret coefficient at high concentrations seems to be a typical phenomena and has also been found for polymer solutions[51] and colloidal dispersions.[52] In the semidilute concentration range the Soret coefficient of the polymeric system shows an asymptotic scaling law with concentration $S_T = C_0 \cdot C^{-0.65}$, whereas the exponent changes from -0.65 to -1 approaching the concentrated regime. For the colloidal system an asymptotic power law for the Soret coefficient S_T in dependence of the volume fraction ϕ of the form $S_T = \phi_0 \cdot \phi^{-0.0095}$ has been found. For the investigated sugar surfactant system the exponent is not temperature independent but decreases from -0.42 to -1.44 with decreasing temperature.

Figure 9 shows the temperature dependence of D_T, D and S_T up to a concentration of w=2.0 wt%. The temperature dependence of S_T is negligible small for concentrations below the *cmc*, for instance w=0.5 wt%, and becomes more pronounced for higher concentrations (2.0 wt%). For sufficiently high concentrations we observe a sign change of S_T from a negative value at low temperatures towards a positive value at higher temperatures. The sign change temperature as well as the slope of the temperature dependence of S_T increases with increasing concentration.

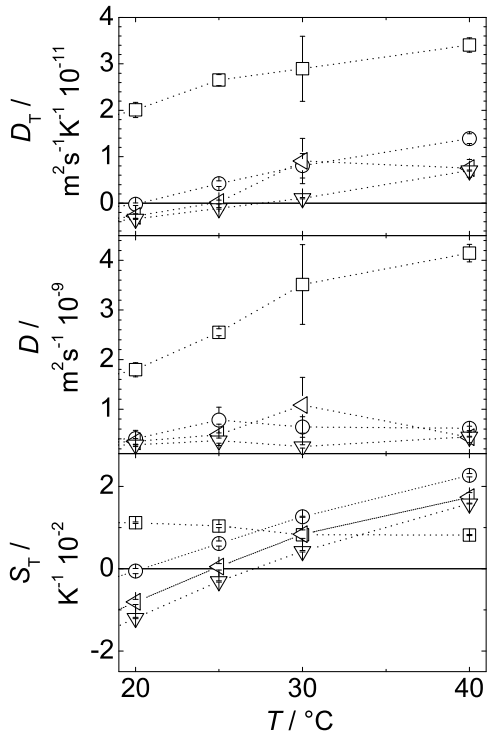

Figure 9: D_T, D, S_T versus temperature in the IR–TDFRS. Concentrations: 0.5 wt% (□), 1.0 wt% (○), 1.5 wt% (◁) and 2.0 wt%(▽).

The sign change from negative to positive S_T-values is a typical behavior of aqueous polymer and colloidal systems.[25,53] Sugaya *et al.*[53] found for aqueous dextran solutions that the temperature dependence was concentration independent. They were able to shift the sign change temperature towards lower temperatures by adding urea, which functioned as a hydrogen bond breaker so the system becomes more "thermophobic" and dextran moves to the cold side. We observe the same trend with increasing temperature when the hydrogen bond formation is weakened. An increase of the sugar surfactant concentration leads to more surface groups interacting via hydrogen bonds and results in a more "thermophilic behavior".

CONCLUSION

We measured the diffusion coefficients and the Soret coefficient of the non ionic sugar surfactant C_8G_1 for different concentrations and temperatures. Special attention has been payed to the region around the critical micelle concentration, which has been determined independently by surface tension measurements.

As expected we find a slower diffusion for the micelles compared to the single sugar surfactant molecules. Although the surface tension measurements indicate that the *cmc* is not influenced by the presence of the dye, we find a pronounced influence of the dye in the thermal diffusion measurements. Below the *cmc* the results for all methods give identical results indicating that the dye diffuses as the sugar surfactant molecules freely in the water. Above the *cmc* we find a much larger value of the Soret coefficient with the classical setup compared to the IR–TDFRS. This effect might be explained by local heating of the dye infected micelles. A similar mechanism might also have led to an abrupt change of the matter lens signal in the work by Santos *et al.*[29] Nevertheless, we find also a change in the slope of the concentration dependence of the Soret coefficient determined with the IR–TDFRS without the dye below and above the critical micelle concentration (cf. Figure 7). One hypothesis in understanding the change of the thermodiffusion behavior near the *cmc* is that the thermo-diffusive motion arises from unbalanced stresses localized

in a thin layer close to the molecule/particle surface, which is primarily determined by the nature and strength of particle/solvent interactions. Following this concept, it seems to be natural to expect a change in the Soret coefficient once micelles are formed, because part of the surfactant molecules are hidden in the inside of the micelles, so that the direct interaction with the solvent is screened.

At higher surfactant concentrations above w=1.0 wt% a sign change has been observed. With increasing temperatures the sign change shifts towards higher concentrations and with increasing concentration the sign change occurs at higher temperatures. The behavior is in analogy with results for concentrated polymeric and colloidal systems and part of the behavior can be explained by the balance of the hydrogen bond formation. We expect that a similar behavior can also be observed for other surfactant systems.

Acknowledgement

The authors thank Reinhard Strey and Jan Dhont for their constant interest in this work and their support. We also appreciate the technical support of Hartmut Kriegs. This work was partially supported by the Deutsche Forschungsgemeinschaft grants So 913 and Wi 1684.

References

(1) He, L. Z.; Garamus, V.; Niemeyer, B.; Helmholz, H.; Willumeit, R. *J. Mol. Liq.* **2000**, *89*, 239–248.

(2) He, L. Z.; Garamus, V. M.; Funari, S. S.; Malfois, M.; Willumeit, R.; Niemeyer, B. *J. Phys. Chem. B* **2002**, *106*, 7596–7604.

(3) *DRP* **1931**, 593422, patent application, E. Th. Böhme AG.

(4) von Rybinski, W.; Hill, K. *Angew. Chem. Int. Ed.* **1998**, *37*, 1328–1345.

(5) Quintero, L. *J. Dispersion Sci. Technol.* **2002**, *23*, 393–404.

(6) Knoche, M. *Weed Res.* **1994**, *34*, 221–239.

(7) Ezrahia, S.; Tuvala, E.; Aserinb, A. *Adv. Colloid Interface Sci.* **2006**, *128-130*, 77–102.

(8) Fischer, E. *Ber. Dtsch. Chem. Ges.* **1893**, *26*, 2400–2412.

(9) Thiem, J. *Tenside Surf. Det.* **1989**, *26*, 324.

(10) Shinoda, K.; Yamaguchi, T.; Hori, R. *Bull. Chem. Soc. Jpn.* **1961**, *34*, 237–241.

(11) Nickel, D.; Nitsch, C.; Kurzendörfer, P.; von Rybinski, W. *Prog. Colloid Polym. Sci.* **1992**, *89*, 249–252.

(12) Kasahara, M.; Hinkle, P. *Proc. Natl. Acad. Sci. USA* **1976**, *73*, 396–400.

(13) Ollivon, M.; Eidelman, O.; Blumenthal, R.; Walter, A. *Biochemistry* **1988**, *27*, 1695–1703.

(14) Vinson, P. K.; Talmon, Y.; Walter, A. *Biophys. J.* **1989**, *56*, 669–681.

(15) Dencher, N. A.; Heyn, M. P. *FEBS Lett.* **1978**, *96*, 322–326.

(16) Michel, H.; Oesterhelt, D. *Proc. Natl. Acad. Sci. USA: Biol. Sci.* **1980**, *77*, 1283–1285.

(17) Polyakov, P.; Wiegand, S. *J. Chem. Phys.* **2008**, *128*, 034505.

(18) Polyakov, P.; Zhang, M.; Müller-Plathe, F.; Wiegand, S. *J. Chem. Phys.* **2007**, *127*, 014502.

(19) Saghir, M. Z.; Jiang, C. G.; Derawi, S. O.; Stenby, E. H.; Kawaji, M. *Eur. Phys. J. E* **2004**, *15*, 241–247.

(20) Wiegand, S. *J. Phys. Condens. Matter* **2004**, *16*, R357–R379.

(21) Kita, R.; Polyakov, P.; Wiegand, S. *Macromolecules* **2007**, *40*, 1638–1642.

(22) Schimpf, M. E.; Giddings, J. C. *Macromolecules* **1987**, *20*, 1561–1563.

(23) Leahy-Dios, A.; Firoozabadi, A. *J. Phys. Chem. B* **2007**, *111*, 191–198.

(24) Piazza, R.; Guarino, A. *Phys. Rev. Lett.* **2002**, *88*, 208302.

(25) Iacopini, S.; Rusconi, R.; Piazza, R. *Eur. Phys. J. E* **2006**, *19*, 59–67.

(26) Ning, H.; Kita, R.; Wiegand, S. *Prog. Colloid Polym. Sci.* **2006**, *133*, 111–115.

(27) Ning, H.; Kita, R.; Kriegs, H.; Luettmer-Strathmann, J.; Wiegand, S. *J. Phys. Chem. B* **2006**, *110*, 10746–10756.

(28) Wiegand, S.; Ning, H.; Kriegs, H. *J. Phys. Chem. B* **2007**, *111*, 14169–14174.

(29) Santos, M. P.; Gomez, S. L.; Bringuier, E.; Neto, A. M. F. *Phys. Rev. E* **2008**, *77*, 011403.

(30) Kutschmann, E. M.; Findenegg, G. H.; Nickel, D.; von Rybinski, W. *Colloid Polym. Sci.* **1995**, *273*, 565–571.

(31) Nilsson, F.; Söderman, O.; Johansson, I. *Langmuir* **1996**, *12*, 902–908.

(32) van Koningsveld, H.; Jansen, J.; Straathof, A. *Acta Crystallogr.* **1988**, *C 44*, 1054–1057.

(33) Pastor, O.; Junquera, E.; Aicart, E. *Langmuir* **1998**, *14*, 2950–2957.

(34) Nilsson, F.; Söderman, O.; Johansson, I. *J. Colloid Interface Sci.* **1998**, *203*, 131–139.

(35) Kita, R.; Wiegand, S.; Luettmer-Strathmann, J. *J. Chem. Phys.* **2004**, *121*, 3874–3885.

(36) Ning, H.; Kita, R.; Wiegand, S. *Prog. Colloid Polym. Sci.* **2006**, *133*, 111–115.

(37) Stubenrauch, C.; Paeplow, B.; Findenegg, G. H. *Langmuir* **1997**, *13*, 3652–3658.

(38) von Szyszkowski, B. *Z. Phys. Chem* **1908**, *64*, 385.

(39) Kriwanek, J.; Lotzsch, D.; Vetter, R.; Seeboth, A. *Polym. Adv. Technol.* **2003**, *14*, 79–82.

(40) Takahashi, Y.; Maeda, A.; Kojima, K.; Uchida, K. *Jpn. J. Appl. Phys., Part 2: Lett.* **2000**, *39*, L218–L220.

(41) Ning, H.; Datta, S.; Sottmann, T.; Wiegand, S. *J. Phys. Chem. B* **2008**, *112*, 10927–10934.

(42) Rosen, M. J. *Surfactants and interfacial Phenomena*, 2nd ed.; Wiley Interscience publication: New York, 1989; p 431.

(43) Preston, W. C. *J. Phys. Colloid Chem.* **1948**, *52*, 84–97.

(44) Strop, P.; Brunger, A. T. *Protein Sci.* **2005**, *14*, 2207–2211.

(45) Lange, H. *Kollid-Z.* **1965**, *201*, 131–136.

(46) Matsson, M. K.; Kronberg, B.; Claesson, P. M. *Langmuir* **2005**, *21*, 2766–2772.

(47) Aoudia, M.; Zana, R. *J. Colloid Interface Sci.* **1998**, *206*, 158–167.

(48) Chen, L. J.; Lin, S. Y.; Huang, C. C.; Chen, E. M. *Colloids Surf., A: Physicochemical and Engineering Aspects* **1998**, *135*, 175–181.

(49) Appell, J.; Porte, G.; Buhler, E. *J. Phys. Chem. B* **2005**, *109*, 13186–13194.

(50) Hogberg, C. J.; Maliniak, A.; Lyubartsev, A. P. *Biophys. Chem.* **2007**, *125*, 416–424.

(51) Rauch, J.; Köhler, W. *J. Chem. Phys.* **2003**, *119*, 11977–11988.

(52) Ning, H.; Buitenhuis, J.; Dhont, J. K. G.; Wiegand, S. *J. Chem. Phys.* **2006**, *125*, 204911.

(53) Sugaya, R.; Wolf, B. A.; Kita, R. *Biomacromolecules* **2006**, *7*, 435–440.

Graphical TOC Entry

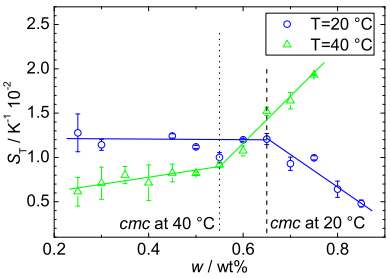

The Soret coefficient S_T at constant temperature versus concentration at 20 °C (○) and 40 °C (△). All measurements have been performed with the IR–TDFRS without dye. The vertical lines mark the *cmc* at 20 °C (dashed) and 40 °C (dotted). The solid lines are guides to the eye.